UV irradiation-induced defect study of GeO_2-SiO_2 glasses by Raman spectroscopy

F. X. Liu
International Center for Materials Physics, Shenyang 110015, People's Republic of China and Structure Research Laboratory and Center for Fundamental Physics, University of Science and Technology of China, Hefei, 230026, People's Republic of China

J. Y. Qian
Department of Physics, University of Science and Technology of China, Hefei, 230026, People's Republic of China

X. L. Wang
Department of Modern Physics, University of Science and Technology of China, Hefei, 230026, People's Republic of China

L. Liu
International Center for Materials Physics, Shenyang 110015, People's Republic of China and Department of Computer Science and Technology, University of Science and Technology of China, Hefei, 230026, People's Republic of China

H. Ming
Department of Physics, University of Science and Technology of China, Hefei, 230026, People's Republic of China
(Received 2 December 1996; revised manuscript received 17 April 1997)

Microstructural changes of two GeO_2-SiO_2 glass compositions (with 5 and 13 mol % GeO_2) irradiated with 5 and 6.4 eV light have been investigated by Raman spectroscopy. The low-frequency ''Boson'' bands at 50 cm^{-1} of both samples shift upward upon irradiation, but their intensities have opposite changes. It indicates that thermal damage of the surface by energetic UV photons is correlated with the Ge content of the glass. The intensities of both defect lines D_1 and D_2 increase with respect to ω_1 and ω_3, and the ω_1 and ω_3 bands shift to higher frequencies which means a reduction of the Si-O-Si bond angle upon irradiation. This may be due to the change in ring statistics in favor of smaller rings, that is, sixfold rings transform to threefold and fourfold rings upon UV irradiation. The opposite changes in intensity of ω_1 and ω_3 bands result from the variation of the network structure. UV photoinduced bond breaking allows structural relaxation of the nonequilibrium glass network that leads to photoinduced Raman changes and the photoinduced index changes in photosensitive glasses. [S0163-1829(97)01130-2]

I. INTRODUCTION

Photosensitivity of germanosilicate glasses became a subject of considerable interest[1–5] since Hill *et al.* discovered the phase grating in GeO_2-doped silica optical fibers photoinduced internally using blue-green light and then Meltz *et al.* discovered the possibility of side writing the grating using UV light. It has opened up the potential of a wide variety of linear and nonlinear optical devices with many applications in communication and sensing technology. Despite the extensive efforts dedicated to explain the growth dynamics of these gratings,[5–8] the microscopic origin of the photorefractivity is not completely understood. Two different mechanisms are usually invoked to account for photoinduced changes in the refractive index. The so-called ''color-center model'' explains index change by the creation of point defects under UV irradiation that modify electronic polarizability.[9] The second model explains change in the refractive index by assuming modifications of the microstructure of the material under UV irradiation.[10] Effects of UV exposure in germanosilicate optical fiber and glass were studied by optical absorption spectroscopy,[11] electron spin-resonance spectroscopy,[12] transmission electron microscopy (TEM), and infrared spectroscopy.[13] Raman spectroscopy has not been used to research this effect up to now. The investigation of the UV-induced microstructural change in GeO_2-SiO_2 glass by Raman-scattering spectroscopy is presented in this work.

II. EXPERIMENT

Two kinds of samples were employed in the experiment: 5% mol. GeO_2-95% mol. SiO_2 and 13% mol. GeO_2-87% mol. SiO_2. These samples were prepared by a modified chemical vapor-deposition (MCVD) process using vapor mixtures of $GeCl_4$ and $SiCl_4$. In this process a porous preform of GeO_2-SiO_2 glass is prepared by depositing the ''Soot'' reaction products (from hydrolysis oxidation of $GeCl_4$-$SiCl_4$ vapor mixtures by a hydrogen-oxygen flame) onto the inside wall of a bait quartz tube rotating in air. This porous preform is then sintered to a high-quality bubble-free glass rod at 1500 °C. The glass composition is controlled by varying the $SiCl_4$ and $GeCl_4$ vapor flows. The GeO_2 content was determined by x-ray energy dispersion techniques as well as deflection rate measurements. This rod was cut into rectangle slabs about $6\times2\times2$ mm.

The ArF (193 nm) and KrF (248 nm) excimer lasers were used for irradiation at room temperature. Their photon ener-

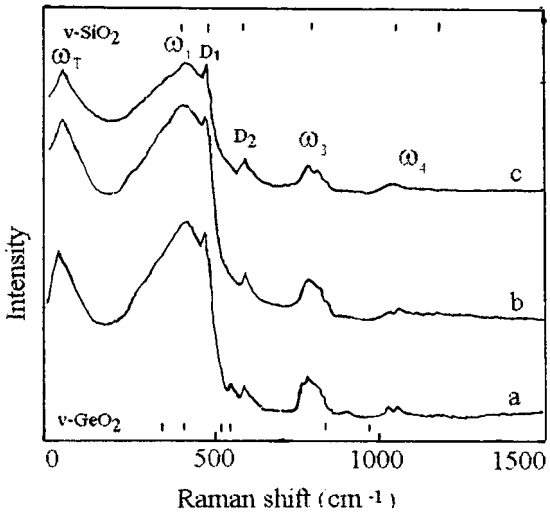

FIG. 1. Stokes-scattered Raman spectra observed in 5% mol germania samples: (a) unirradiated sample, (b) sample irradiated with a 5.0-eV photon, (c) sample irradiated with a 6.4-eV photon.

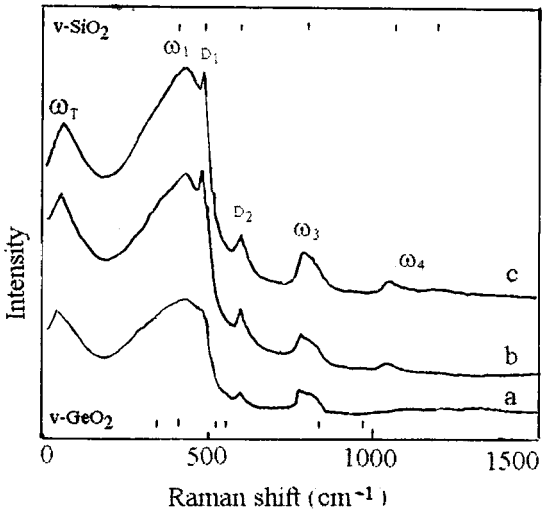

FIG. 2. Stokes-scattered Raman spectra observed in 13% mol germania samples: (a) unirradiated sample, (b) sample irradiated with a 5.0-eV photon, (c) sample irradiated with a 6.4-eV photon.

gies are 6.4 and 5.0 eV, respectively. The excimer lasers were operated at 20 Hz with a $\sim$20 ns pulse width. Their output beams had a 6 mm height, a 2 mm width, and 500 mJ/cm^2 pulse intensity. Each kind of glass sample is subjected to different kinds of irradiation. Duration of exposure is 5 min. for all.

Room-temperature Raman-scattering spectroscopy was used to ascertain the structural changes of the glass samples. Raman spectra were obtained from a SPEX-1403 Raman spectrometer and data acquisition was controlled by a SPEX datamater computer. Sample excitation was achieved using the 514.5 nm line of an argon-ion laser with 200-mW power. Scattering radiation was collected at 90° to the excitation beam.[14]

III. RESULTS AND DISCUSSIONS

After irradiation, the samples had a distinctive surface deep gray color resulting from a local densification of the UV-irradiated glass and the formation of color centers. More recently, Bragg grating similar to ours written in the same material has been investigated by TEM. Surface level modulation associated with the grating shows that densification has been induced by UV irradiation.[13] Thus, there is now a large body of compelling evidence that demonstrates that inscription of Bragg grating in germanosilicate glasses induces glass compaction.

The representative Stokes-scattered Raman spectra of unirradiated sample (a), sample irradiated with a 5.0-eV photon energy (b), and sample irradiated with a 6.4-eV photon (c) are shown in Figs. 1 and 2, as measured. The spectra have been shifted vertically to facilitate comparison. The major Raman spectral features exhibited in pure SiO_2 and pure GeO_2 glasses can be seen in the figure for comparison.

In all samples, features of the pure silica spectrum are still evident, including a shoulder at approximately 490-cm^{-1} reminiscent of the D_1 silica band and a sharp line at 602 cm^{-1} corresponding to the D_2 band. D_1 and D_2 ''defect'' lines have been interpreted by Galeener to correspond to the symmetric stretch (SS) vibration of oxygen in a regular (possibly puckered) tetrasiloxane and trisiloxane ring structure.[15,16] The dominant (Raman-active) ring mode frequencies decrease with increasing ring order. The bands have decreased in intensity and broadened when compared with those of a pure v-SiO_2 Raman spectrum.[17] The broad features are labeled ω_1, ω_3, ω_4(TO), and ω_4(LO) for reasons discussed in Ref. 18. They have been identified with vibrations of the glass network as described by a nearest-neighbor central-force dynamic theory. Compared with those of a pure v-SiO_2 Raman spectrum, these features are broadened because the Si-O-Si bond angles in that network are widely distributed.

Because there is a greater population of thermally exited low-energy phonons at room temperature,[19] the 50-cm^{-1} band (ω_T) has been assigned to the ''Boson'' band. And the Raman spectra are enhanced at the low-frequency region between 432 and 50 cm^{-1} compared with the predictions of microscopic models for structural and vibrational response.

Following UV irradiation, strong changes in the Raman spectrum were measured. Figure 1 indicates that the low-frequency ''Boson'' band at 50 cm^{-1} shifts upward to 65 cm^{-1} after 6.4 eV photon irradiation. When photon energy increases a pronounced change is observed of the shape and intensity in the broad continuous region between 432 and 50 cm^{-1}. These are caused by thermal damage of the surface by energetic UV photons. UV-induced surface damage causes an increase in Rayleigh scattering near the exciting line that intensifies as a function of photon energy. The photoinduced processing with UV light generally takes place under the extreme conditions of a high-energy UV laser pulse. During each pulse, the new network developed from the previous pulse is shaken up and then frozen. It follows that such a network will evolve, if possible, to a state that attempts to minimize the buildup of stress during the pulse. UV light would break wrong bonds first induces relaxation of the internal stresses introduced during processing of the fiber or the preform. Then, the glass would evolve towards a more stable, denser state and would finally lead to

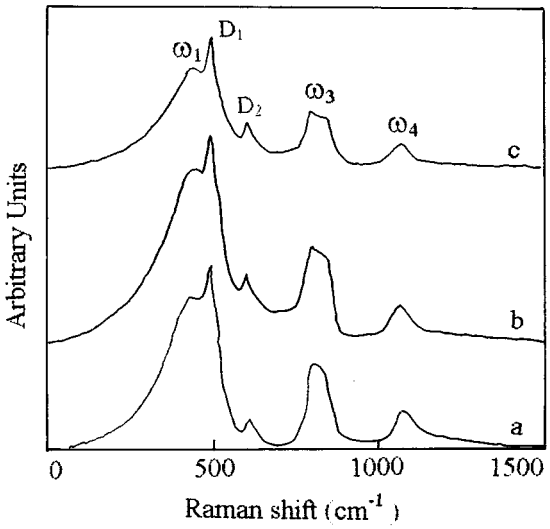

FIG. 3. Reduced Raman spectra of 5% mol germania samples: (a) unirradiated sample, (b) sample irradiated with a 5.0-eV photon, (c) sample irradiated with a 6.4-eV photon.

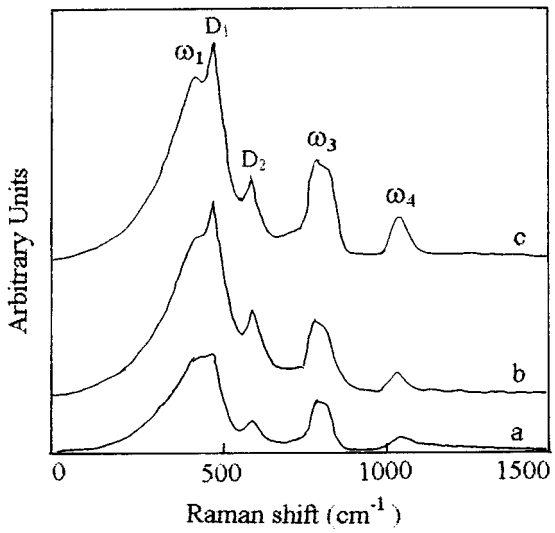

FIG. 4. Reduced Raman spectra of 13% mol germania samples: (a) unirradiated sample, (b) sample irradiated with a 5.0-eV photon, (c) sample irradiated with a 6.4-eV photon.

a glass network with a medium-order similar to that of α quartz, the stable crystalline form of silica at room temperature.[10]

Figure 2 shows the Stokes-scattered Raman spectra observed in 13% mol germania samples: (a) unirradiated sample, (b) sample irradiated with a 5.0-eV photon, (c) sample irradiated with a 6.4-eV photon. The low-frequency ''Boson'' scattering band at 45 cm^{-1} shifts upward to 68 cm^{-1} at a 6.4-eV photon. The change of shape and intensity was in contrast to that of Fig. 1. This means that the thermal damage of the surface by energetic UV photons is correlated with the Ge content of the glass.

The raw spectra in Figs. 1 and 2 must be reduced in order to eliminate extraneous temperature dependencies and compare most meaningfully the effects of irradiation with different UV photon energies on the microstructure of GeO_2-SiO_2 glasses.

The reduced Raman spectra are calculated from the direct spectra $I^P(\omega_L,\omega_S)$ viz. Figs. 1 and 2 according to[19]

$$I^P_{\rm red}(\omega)\equiv I^P(\omega_L,\omega_S)(\omega_L-\omega)^{-4}\omega[n(\omega)+1]^{-1}, \quad (1)$$

where ω_L is the frequency of the incident (laser) light, and $\omega_S\equiv\omega_L-\omega$ is the frequency of the scattered light. Thus, ω is the phonon frequency while $-\omega$ is the Raman shift for the Stokes spectrum (creation of a phonon, as in Figs. 1 and 2). Here

$$n(\omega)\equiv[\exp(\hbar\omega/k_BT)-1]^{-1} \quad (2)$$

is the Bose-Einstein occupation number for sample temperature T. The results of applying these data reduction procedures to Figs. 1 and 2 are shown in Figs. 3 and 4.

Comparing the Raman spectra of unirradiated 13% mol germania glass [Fig. 4(a)] with that of unirradiated 5% mol germania glass [Fig. 3(a)] the influence of increased germania content is readily observed. The major peak, previously centered at 432 cm^{-1} attributed to V_s(Si-O-Si) symmetric stretching mode in the lower germania content glass, has shifted to approximately 436 cm^{-1} and narrowed. This is in agreement with previous melt pure germania spectrum that is reported to exhibit a narrow band owing to the analogous Ge-O-Ge symmetric-stretching vibration at approximately 416 cm^{-1}.[20] With increasing GeO_2 content, the intensity of the D_1 line decreases sharply, while that of the D_2 line decreases. These have been interpreted as a reduction in the stability of the four- and three-membered ring structures with the substitution of Ge for Si into the v-SiO_2 network.[21,22] The $\sim$800-cm^{-1} envelope, which is a doublet composed of bands at 797 (TO) and $\sim$830(LO) cm^{-1} becomes weaker, broader, and planar. This is just the result of the increase of the Ge content. The decrease of the intensity implies that the concentration of the Si-Ge wrong bonds increase with the Ge content and the formation of Ge-O-Si bridging bonds.[10]

Figures 3 and 4 show that that intensities of both D_1 and D_2 defect lines in the glasses of two different Ge contents increase with respect to ω_1 and ω_3 upon irradiation.

The anomalous changes of the sample in Fig. 3(b) are due to the strong absorption of 248 nm light by the glass. We note that the planar rings with lowest energy E_n (activation energy) are first fourfold then threefold. Because the threefold ring defects have a higher activation energy[18] (Galeener estimated a formation energy of 0.16 eV for fourfold planar ring defects and 0.51 eV for threefold planar ring defects) and has a smaller volume than the fourfold ring, we can expect that there will be fewer fourfold ring defects than threefold rings in the glass. These differences explain the fact that there is a sharp increase in D_1 line intensity but a relatively small increase in the D_2 line intensity.

TABLE I. Frequencies of the relative maxim of the first-order 5% mol GeO_2 glass Raman spectra as a function irradiation photon energy.

E_p (eV)	ω_T (cm^{-1})	ω_1 (cm^{-1})	ω_3 (cm^{-1})	ω_4 (TO) (cm^{-1})	ω_4 (LO) (cm^{-1})	D_1 (cm^{-1})	D_2 (cm^{-1})
0	50	432	800	1060	-	490	602
5.0	55	436	806	1058	-	491	603
6.4	65	438	808	1055	1065	492	604

Tables I and Tables II show the measured frequencies of Raman spectral features observed in GeO_2-SiO_2 glasses with different Ge content as a photon energy E_p. The error in all frequency measurements is estimated to be ± 1.5 cm^{-1}.

We make two statements with regard to the defect-line frequency behavior. First, most of the correlation of the D_1 defect line with photon energy may be due to its proximity to the much stronger main line ω_1, therefore, D_i frequency may be entirely independent of photon energy. Second, the D_1 and D_3 frequencies have been found to be independent of Si and Ge atomic masses, as demonstrated by isotopic substitution experiments. The stability of these frequencies is consistent with their assignment to the SS mode of regular ring defects.

The intensities ω_1 and ω_3 have opposite changes: that of 5% mol GeO_2 glass descends upon irradiation and that of 13% mol GeO_2 glass ascends. Figures 3 and 4 also show that the ω_4 band of both glasses shifts to a lower frequency side, but the intensities have opposite changes.

The oxygen-deficient bonds that are adjacent to Si-O or Ge-O bonds are the weakest bonds in a pure germanosilicate glass matrix. This is because the electronegativity of oxygen is larger than that of the Si or Ge atoms. In other words the Si or Ge atoms in these bonds have their bonding orbital electrons localized towards the Si-O or Ge-O bonds. This means that they are stretched or under local strain and therefore are relatively weak and easier to break. However, there is another process—that of the breakup of the Ge-Si wrong bond. The Ge-Si wrong bonds are responsible for photosensitivity of MCVD germanosilica glass.

Germania, like silicon, has a moderately stable $+2$ oxidation state, and the suboxide GeO becomes more stable than GeO_2 at high temperature. This is of importance in fiber preform fabrication since incorporation of GeO produced during the high-temperature gas phase oxidation process of the MCVD results in an oxygen-deficient matrix and forms Ge-Si wrong bonds. The mixing of GeO_2 and SiO_2 results in a continuous random network structure of TO_4 tetrahedral ($T=$ Si, Ge) in the glass. In addition to formation of Si-O-Ge bonds there is a considerable degree of Si-Ge wrong bonds.

The Ge-O and Ge-Si bonds are weaker than Si-O bonds. They can be readily broken by low-energy radiation (UV, x-ray radiation, and low-energy electrons).

The larger bond length increase between the Ge and Si atoms under irradiation follows ionization of the Ge-Si wrong bond. The separation of the Ge and Si atoms is too large for immediate rebonding to give the Ge-Si wrong bond. This is a reasonable suggestion because the breaking of the Ge-Si bonds leads to a GeE′ center accompanied by a large lattice relaxation, which is expected to stabilize the GeE′ centers by preventing recombination and forming some ring defects and network.

Given the preponderance of Ge-Si bonds over Si-Si bonds, it is not a surprise that germanosilica glass is considerably more susceptible to radiation damage than pure silica.

UV light is strongly absorbed by germanosilicate glasses and we can assume that many wrong bonds are broken and reformed, or Si-O-Ge bonds are formed during irradiation. The UV irradiation process is a competitive one between the increase of the network structure resulting from the formation of Si-O-Ge bonds and the decrease of the network structure resulting from the breakup of the wrong bonds. The Ge-Si wrong bond increases with the Ge content. The former process is dominant, so in the high Ge content glass there appears the increase in the intensity of network vibrational modes ω_1, ω_3, and ω_4.

In the lower Ge content glass, there are also two processes. Since the Ge-Si wrong bonds are relatively few and the available population is depleted, the breakup of the network structure is dominant, which leads to the decrease of the intensity of network vibrational modes ω_1, ω_3, and ω_4.

We also see that both ω_1 and ω_3 bonds have shifted to the higher-frequency sides.

The ω_i frequencies are predicted to be dependent upon the Si-O-Si bridging bond angle θ by a central-force idealized continuous-random-network (CF-ICRN) theory.[18] Their frequencies are given by the equations

$$\omega_1^2=(\alpha/m_{\mathrm{O}})(1+\cos\theta), \tag{3}$$

TABLE II. Frequencies of the relative maxim of the first-order 13% mol GeO_2 glass Raman spectra as a function irradiation photon energy.

E_p (eV)	ω_T (cm^{-1})	ω_1 (cm^{-1})	ω_3 (cm^{-1})	ω_4 (TO) (cm^{-1})	ω_4 (LO) (cm^{-1})	D_1 (cm^{-1})	D_2 (cm^{-1})
0	45	436	800	1054	1070	490	604
5.0	50	440	806	1050	1068	490	604
6.4	68	444	810	1048	1065	492	604

TABLE III. Total change in the bridging oxygen bond angle θ predicted by Eqs. (3)–(6) for UV irradiated SiO_2-GeO_2 glasses.

Network feature	UV irradiated of 5% mol Ge glass (unirradiated vs 193 nm)		UV irradiated of 13% mol Ge glass (unirradiated vs 193 nm)	
	$\Delta\omega_{\text{total}}$ (cm^{-1})	$\Delta\theta$ (deg)	$\Delta\omega_{\text{total}}$ (cm^{-1})	$\Delta\omega$ (deg)
ω_1	6	−0.69	8	−0.93
ω_3	8	−0.91	10	−2.1
ω_4(TO, LO)	−5	−1.4	−6	−1.7

$$\omega_3^2=(\alpha/m_{\text{O}})(1+\cos\theta)+(4\alpha/3m_{\text{Si}}), \tag{4}$$

$$\omega_4^2=(\alpha/m_{\text{O}})(1-\cos\theta)+(4\alpha/3m_{\text{Si}}). \tag{5}$$

Here, ω_i are the angular frequencies (in rad/sec) while m_{O} is the mass of the oxygen atom; m_{Si} is the mass of the silicon, α is the Si-O bond-stretching force constant. (All other force constants are assumed to be zero.) For small changes in θ, we can relate $\Delta\theta$ to $\Delta\omega_i$ by differentiating Eqs. (3)–(5) to obtain

$$\Delta\omega_i=\pm(\alpha/m_0)\sin\theta\Delta\theta/2\omega_i, \tag{6}$$

where the sign is negative for $i=1$ and 3, and positive for $i=4$. Equations (3)–(6) elucidate the changes in ω_i with photon energy, in particular the opposite sign of the $\omega_{1,3}$ and ω_4 shifts. Densification of the network with increasing photon energy E_p would reduce the average value of θ, and therefore $\Delta\theta$ in Eq. (6) must be negative and $\Delta\omega_i$ is positive for ω_1 and ω_3 and negative for ω_4. Here, we use $\alpha=535$ N/m and $\theta=130°$.[18]

Table III shows the result of applying these equations to the total frequency shifts observed between unirradiated and 193-nm irradiated materials for two different Ge content glasses.

It has been suggested that the asymmetry in the 437-cm^{-1} band may be due to the presence of high-membered ($n>4$) rings of SiO_4 tetrahedra in the glass.[23] In fact, a molecular-dynamics simulation of Rino *et al.*[24] indicates that SiO_4 tetrahedra organize in n-fold rings with $3\leqslant n\leqslant 10$, $n=6$ being the most frequent value in both amorphous and molten silica. Galeener concluded that whenever an n-fold ring is formed in a glass, it attempts to minimize its energy of the glass by relaxing its Si-O-Si bond angles towards the lowest energy (or most probable) value $\langle\theta\rangle$.[15] So, both intensities of the D_i defect lines increase relative to that of network mode ω_1 and the reduction of the Si-O-Si bond angle (θ) upon irradiation may be due to the change in ring statistics in favor of smaller rings, that is, six-fold rings transform to three-fold and four-fold rings upon UV irradiation.

IV. CONCLUSIONS

In summary, we have investigated the changes in Raman spectrum as a function of UV irradiation photon energy and related them to microstructure modification of the GeO_2-SiO_2 network. UV-induced surface damage causes an increase in Rayleigh scattering near the exciting line that intensifies as a function of photon energy. For different Ge content glass we have observed different changes in the intensity and the frequency of various modes. First, the intensities of both D_1 and D_2 defect lines in the glasses of different Ge content increase with respect to ω_1 and ω_3 upon irradiation. Second, for all irradiated glasses, we observed the blue-shifts in frequencies of the host-network vibration modes ω_1 and ω_3, but smaller or no change in the frequencies of the two defect modes. The shifts of the network mode frequencies are related to the reduction in the T-O-T ($T=$ Si, Ge) bridge bond angle θ for irradiated glasses, by the central-force idealized continuous-random-network (CF-ICRN) theory, suggesting the change in ring statistics in favor of smaller rings, viz., six-fold rings transform to three-fold and four-fold rings upon UV irradiation.

The intensities of the ω_1 and ω_3 bands have opposite changes: that of 5% mol GeO_2 glass descends upon irradiation and that of 13% mol GeO_2 glass ascends. The ω_4 band of both glasses has shifted to the lower-frequency side, but the intensities have opposite changes. So, the Ge content may affect a lot for the optical fiber writing of photosensitive materials. This means that the UV irradiation process is a competitive process between the increase of the network structure from the formation of Si-O-Ge bonds and the decrease of the network structure from the breakup of the wrong bonds.

In germanosilica fibers, the photoinduced process is triggered by breaking of Ge-Si wrong bonds introduced during the MCVD process.

Although the exact nature of the above Raman features is unclear, it is confirmatively attributed to the changes of defects. From this point, the microscopic origin of the photosensitivity in irradiated germanosilicate fibers can be understood as a structural modification of the glass under irradiation due to the formation of some permanent defect states.

ACKNOWLEDGMENTS

The authors would like to thank Professor Yinshan Yu and Dr. Fangdong Wu of Anhui Institute of Optics and Fine Mechanics for their help in the experiment, Professor C. Y. Xu and J. Zuo for their assistance in obtaining the Raman spectra. The authors also wish to thank Yuan Xu of Wuhan Post and Telecommunication Research Institute, Optical Fiber Division, for supplying the GeO_2-SiO_2 glasses. This work was supported by National Natural Science Foundation of China, Grant No. 19174053.

[1] K. O. Hill, Y. Fujii, D. C. Johnson, and B. S. Kawasaki, Appl. Phys. Lett. **32**, 647 (1978).
[2] G. Melz, W. W. Morey, and W. H. Glenn, Opt. Lett. **14**, 823 (1989).
[3] G. Q. Zhang, S. M. Liu, J. J. Xu, and Q. Y. Zhang, Phys. Lett. A **204**, 146 (1995).
[4] Z. X. Li, D. Ning, H. Li, J. P. Zhou, and W. M. Liu, Acta Phys. Sin. **41**, 890 (1992).
[5] F. X. Liu, C. H. Zhang, and Z. M. Li, Nucl. Tech. (China) **17**, 51 (1994).
[6] P. St. J. Russell and D. P. Hand, Electron. Lett. **15**, 102 (1990).
[7] I. Abdulhalim, Appl. Phys. Lett. **66**, 3248 (1995).
[8] T. E. Tsai and D. L. Griscom, Proc. SPIE **1516**, 14 (1991).
[9] L. Dong, J. L. Archambault, L. Reekie, P. St. J. Russell, and D. N. Payne, Appl. Opt. **34**, 3436 (1995).
[10] M. G. Sceat and P. A. Krug, Proc. SPIE **2044**, 113 (1993).
[11] V. B. Neustruev, J. Phys., Condens. Matter. **6**, 6901 (1994).
[12] T. E. Tsai, E. J. Friebele, and D. L. Griscom, Opt. Lett. **18**, 935 (1993).
[13] P. Cordier, J. C. Doukhan, E. Fertein, P. Bernage, P. Niay, J. F. Bayon, and T. Georges, Opt. Commun. **111**, 269 (1994).
[14] F. X. Liu, Y. S. Wu, and Y. T. Qian, Acta Opt. Sin. **12**, 946 (1992).
[15] F. L. Galeener, Solid State Commun. **44**, 1037 (1982).
[16] F. L. Galeener and A. E. Geissberger, Phys. Rev. B **27**, 6199 (1983).
[17] F. L. Galeener, J. Non-Cryst. Solids **71**, 373 (1985).
[18] F. L. Galeener, Phys. Rev. B **19**, 4292 (1979).
[19] F. L. Galeener, A. J. Leadbetter, and M. W. Stringfellow, Phys. Rev. B **27**, 1052 (1983).
[20] S. K. Sharma, D. W. Matson, J. A. Philpotts, and T. L. Roush, J. Non-Cryst. Solids **68**, 99 (1984).
[21] N. Xiao, Z. Xu, and D. Tian, J. Phys. Condens. Matter **1**, 6343 (1989).
[22] F. X. Gan, G. S. Huang, and S. Z. Chen, J. Non-Cryst. Solids **52**, 203 (1982).
[23] S. K. Sharma, J. F. Mammone, and M. F. Nicol, Nature (London) **292**, 140 (1981).
[24] J. P. Rino, I. Ebbsjo, R. K. Kalia, A. Nakano, and P. Vashishta, Phys. Rev. B **47**, 3053 (1993).